The polyproline II conformation in short alanine peptides is noncooperative

Kang Chen, Zhigang Liu, and Neville R. Kallenbach†

Department of Chemistry, New York University, New York, NY 10003

Communicated by Robert L. Baldwin, Stanford University Medical Center, Stanford, CA, September 8, 2004 (received for review July 15, 2004)

The finding that short alanine peptides possess a high fraction of polyproline II (PII) structure ($\Phi = -75°$, $\Psi = +145°$) at low temperature has broad implications for unfolded states of proteins. An important question concerns whether or not this structure is locally determined or cooperative. We have monitored the conformation of alanine in a series of model peptides AcGG(A)nGGNH$_2$ (n = 1–3) over a temperature range from −10°C to +80°C. Use of ^{15}N-labeled alanine substitutions makes it possible to measure $^3J_{\alpha N}$ coupling constants accurately over the full temperature range. Based on a 1D next-neighbor model, the cooperative parameter σ of PII nucleation is evaluated from the coupling constant data. The finding that σ is close to unity (1 ± 0.2) indicates a noncooperative role for alanine in PII structure formation, consistent with statistical surveys of the Protein Data Bank that suggest that most PII structure occurs in isolated residues. Lack of cooperativity in these models implies that hydration effects that influence PII conformation in water are highly localized. Using a nuclear Overhauser effect ratio strategy to define the alanine Ψ angle, we estimate that, at 40°C, the time-averaged alanine conformation ($\Phi = -80°$, $\Psi = +170°$) deviates from canonical PII structure, indicating that PII melts at high temperature. Thus, the high-temperature state of short alanine peptides seems to be an unfolded ensemble with higher distribution in the extended β structure basin, but not a coil.

Because many proteins are suspected to be weakly folded *in vivo*, the characteristics of unfolded states of proteins are becoming of considerable interest (reviewed in ref. 1). Recent research has uncovered several surprising features of the structure in unfolded peptides and proteins (reviewed in ref. 2). Rather than the statistical coil expected from analysis of the dimensions of unfolded proteins in solvent such as guanidine hydrochloride (3), unfolded proteins seem to be locally ordered, with substantial amounts of polyproline II (PII) structure. PII is a left-handed 3_1 helical structure occupied by collagen and peptides containing proline with dihedral angles $\Phi = -75°$ and $\Psi = +145°$. Unfolded structures of peptides in native folding conditions can be studied by using chains too short to nucleate normal α-helix or β-strand structure; these chains have the advantage of being amenable to theoretical as well as experimental analysis. A wealth of spectroscopic and theoretical evidence indicates that oligomers of two or three alanines, the simplest models for the peptide backbone, have predominantly PII conformation in water (4–9). Similarly, the single alanine residue in the pentapeptide AcGGAGGNH$_2$ (GGAGG) is predominantly PII in water at 20°C (10). The glycines flanking alanine in this pentapeptide have the maximal possible conformational freedom for peptide bonds. This and related model peptides have been used to represent unfolded backbone protein structure for many years (11–13). The solvent trifluoroethanol (TFE) has been widely used as an α-helix-stabilizing agent (14, 15). When the solvent is changed from water to neat TFE, PII structure disappears, judging from the CD spectrum (16). NMR analysis of the alanine dihedral angles of GGAGG in TFE shows that an internally H-bonded C7eq turn conformation is favored over PII or α structure (16). The C7eq structure is found to be most stable in calculations on alanine dipeptide *in vacuo* (17, 18). There is thus evidence for a role of solvation in maintaining PII structure, a point that has been emphasized in many articles and reviews since it was first suggested by Tiffany and Krimm (19). PII structure has been associated with highly hydrated regions in native proteins (20). The x-ray crystal structures of model collagen peptides reveal nets of water-bridged hydrogen bonds coating the PII-helix surface (21). Theoretical calculations on alanine dipeptide have been interpreted to imply that PII structure is stabilized by water hydrogen bonding to backbone amide nitrogen and carbonyl oxygen (22). A rather different view is that PII conformation least disrupts the H-bonding patterns present in liquid water (23, 24). Whatever the detailed mechanism of interaction of water with the peptide backbone, it is possible that residues adjacent to those with PII structure will tend also to favor PII conformation. Cooperative effects attending PII formation might then arise, with important consequences for early stages in protein folding. The question we address here is whether or not formation of PII structure is cooperative (6, 9).

Because alanine provides a minimal model for the isolated peptide chain (glycine is anomalous in its flexibility), we focus on the properties of alanine peptides. In a previous NMR and CD study of AcX$_2$A$_7$O$_2$NH$_2$ (X$_2$A$_7$O$_2$), an alanine heptamer flanked by short basic residues for solubility (X, diaminobutyric acid; O, ornithine), each of the seven alanines in the peptide was found to be predominantly in PII at low temperatures (25). Whereas this finding is not inconsistent with cooperativity in forming PII, statistical surveys indicate that some 80% of the PII conformation in native proteins from the database occur as isolated residues (26), suggesting that cooperativity may be much weaker than in α-helices, for example. Inspection of the extended 3_1 left-handed PII-helix implies that side chain–side chain interactions should be minimal. Local steric effects (27) may influence PII cooperativity by excluding conformational space to compact structures in addition to the role of solvent discussed above. Cooperative effects in the conformation of alanine in model peptides are analyzed here by using a series of models AcGG(A)nGGNH$_2$ with n = 1, 2, and 3 (abbreviated as GG(A)nGG). ^{15}N labeling is used to isolate individual alanines in the series for NMR analysis. We find essentially noncooperative behavior in these peptides using a simple next-neighbor model to quantify the extent of cooperativity present.

Materials and Methods

Theory of Transition Between PII and "U." We apply an Ising model (28) to analyze the potential extent of cooperativity in the peptides. The assumption is that only P (PII structure, low temperature folded) and U (denoting the thermally unfolded ensemble of alanine >80°C) states are accessible to any given alanine residue in GG(A)nGG over the temperature ranging from 0°C to 80°C.

The formation of an isolated alanine in PII is governed by the equilibrium equation:

Abbreviations: PII, polyproline II; NOE, nuclear Overhauser effect.

†To whom correspondence should be addressed. E-mail: nrk1@nyu.edu.

www.pnas.org/cgi/doi/10.1073/pnas.0406657101

$$U \overset{K_{up1}}{\longleftrightarrow} P.$$

The fractional content of each conformation is given by

$$f_U = (J_{(T)} - J_P)/(J_U - J_P), f_U + f_P = 1. \quad [1]$$

Measured $^3J_{\alpha N}$ coupling constants are abbreviated in Eq. **1** as $J_{(T)}$, which is temperature-dependent. *Jp* and *Ju* represent the coupling constants corresponding to 100% *P* and *U* states, respectively, values of which are estimated from the experimental transition data; *f* is the fraction of each conformation at a given temperature. The equilibrium constant K_{up1} at different temperatures can be calculated by Eq. **2** below.

$$K_{up1} = fp/fu \quad [2]$$

so that, according to the van't Hoff equation

$$-R \ln K_{up1} = \Delta G_{up1}/T = \Delta H_{up1}/T - \Delta S_{up1} \quad [3]$$

the transition enthalpy ΔH_{up1} and entropy ΔS_{up1}, both assumed to be temperature-independent, can be calculated. ΔG_{up1} is the transition free energy. As additional alanines are introduced, the number of conformational states increases. In the case of two adjacent alanines, there are four states, designated as *UU*, *UP*, *PU*, and *PP*. The equilibrium between states of adjacent alanines designated by conformations *UP* or *PU* and *PP* has a constant K_{up2} different from K_{up1} because of potential cooperativity.

$$UP \overset{K_{up2}}{\longleftrightarrow} PP$$

$$-R \ln K_{up2} = \Delta G_{up2}/T = \Delta H_{up2}/T - \Delta S_{up2} \quad [4]$$

The quantities σ and *s* are defined in Eq. **5**.

$$s = K_{up2}, \quad \sigma = K_{up1}/K_{up2} \quad [5]$$

If $K_{up1} < K_{up2}$ and $\sigma < 1$, the *U–P* transition is positively cooperative. For α-helix, σ is below 10^{-2} (29). If $\sigma = 1$, there is no difference between K_{up1} and K_{up2}, and no cooperativity.

The partition function of a given chain sums the statistical weights of all accessible states and can be computed in terms of the equilibrium constants represented by σ and *s*, usually by setting the weight of the *UU* state to be unity as a reference. The matrix Eq. **6** allows calculation of the partition function *Qn* for a peptide with *n* continuous alanines (28). *W(iP)* represents the statistical weight of conformations with *i* of the number residues in PII.

$$Qn = \sum_{i=0}^{n} W(iP) = (1, 0)\begin{pmatrix} 1 & \sigma s \\ 1 & s \end{pmatrix}^n \begin{pmatrix} 1 \\ 1 \end{pmatrix} \quad [6]$$

Peptide Synthesis and Purification. Peptides GG(A)nGG (n = 1–3) were assembled on Rink amide resin (Advanced ChemTech) with a RAININ Instrument PS3 solid phase synthesizer using Fmoc (9-fluorenylmethyloxycarbonyl) chemistry. Fmoc-Ala/Gly, the coupling reagent HBTU (2-(1*H*-benzotriazol-1-yl) 1,1,3,3-tetramethyluroniumhexafluoro phosphate) and HOBT (*N*-hydroxybenzotriazol) were purchased from Nova Biochem. ^{15}N-labeled Fmoc-Ala was purchased from Isotech (St. Louis) The N terminus of each peptide was capped with acetic anhydride after its assembly on the solid matrix. Cleavage of peptides from the resin was performed with 95% trifluoroacetic acid (TFA) in the presence of the scavenger 2.5% TIS (triisopropylsilane) and 2.5% H_2O. After precipitation with cold ether, the crude peptide product was dissolved in trifluoroethanol/TFA (vol. 1:1) and vigorously shaken for 5 h. The sample was purged with nitrogen gas overnight to remove solvent. Samples were purified on a reverse-phase HPLC C-18 preparative column (2.2 × 25 cm, 300 Å, Grace Vydac, Hesperia, CA) with water and acetonitrile as eluents. Fractions containing product were pooled and lyophilized. The molecular weight of each peptide was confirmed by a matrix-assisted laser desorption/ionization time-of-flight (MALDI-TOF) mass spectrometer (Bruker, Billerica, MA).

CD Spectroscopy and Peptide Concentration Determination. Far UV CD spectra were recorded on an AVIV 202 CD spectrometer by using 0.1-cm pathlength CD cuvettes (Hellma QS, Hellma, Forest Hills, NY). The wavelength scan ranged from 190 to 260 nm. Measurements were carried out with 0.5- to 1-mM peptide in 20 mM potassium phosphate buffer with pH adjusted to 3.5. Temperature was varied from −10°C to 90°C with 10°C increments. Four scans were averaged at each temperature. All CD spectra shown have the solvent baselines subtracted. The peptide concentration was determined by a combination of UV absorbance and NMR peak integration. Briefly, the CD sample solution was mixed with a tryptophan stock solution, having a known concentration measured from its UV 280 nm absorbance ($\varepsilon_{280\ nm}$ = 5,690 $M^{-1}\cdot cm^{-1}$). A 1D NMR spectrum was recorded on the mixed sample. The β protons of Trp (≈3.2 ppm) and those of the corresponding β protons of the acetyl protection group of each peptide (≈2.0 ppm) were integrated to give a quantitative ratio, from which the peptide concentration could be calculated.

NMR Spectroscopy. All NMR experiments were performed on a Bruker AVANCE 500-MHz spectrometer equipped with an inverse triple resonance 5-mm TX1 probe and a GRASP III gradient accessory. The carrier frequency was set to the water resonance in all experiments. Temperature was controlled by means of a BVT3200 thermo unit. The reported temperature was calibrated by using either 100% methanol (<35°C) or 80% ethylene glycol/20% DMSO (>35°C). NMR samples were prepared with 2–3 mM ^{15}N-labeled peptide dissolved in the same buffer used in CD experiments with the addition of 10% ^2H_2O for locking. All 1D high-resolution experiments were recorded with 64,000 complex data points collected and 32 scans averaged at a spectra width of 6,000 Hz by using a Bruker watergate pulse sequence ZGGP3919 (30). The original free induction decay (FID) was zero-filled to 128,000 points and Fourier transformed without any weighting function applied. The coupling constant values were derived from the Gaussian deconvolution algorithm provided in XWINNMR 3.5 (Bruker). The standard deviation from Gaussian peak fitting was propagated to estimate the $^3J_{\alpha N}$ coupling constant experimental error. Data collection and process were consistent within all 1D measurements.

The 1D spectrum of the proton (spin ½) attached to ^{14}N (spin 1) should be a triplet with frequencies $\omega_H(M') = -\gamma_H B_0 + J_{1H-14N}M', M' = -1,0,1$. Due to fast relaxation of ^{14}N (T1 ≈ ms) (31), the jumping rate between ^{14}N energy levels is faster than J_{1H-14N} (≈50 Hz), so the triplet peaks coalesce to a single peak at the average frequency $-\gamma_H B_0$ (32). Thus, the normally observed amide proton peaks are split by the α proton to give a doublet. A brief calculation based on Pople's line shape equation shows that the amide proton linewidth increases from 4.0 to 20 Hz as the T1 relaxation time of ^{14}N changes from 1.1 to 5.4 ms with increasing temperature (33). The extreme line broadening of natural amide proton peak limits conventional $^3J_{\alpha N}$ measurements (4–10 Hz) at higher temperatures. However, replacement of ^{14}N with ^{15}N removes the quadrupolar effect efficiently and gives less overlap with other ^{14}N amide proton peaks when ^{15}N decoupling is not applied (see Fig. 2*D*). This result makes it

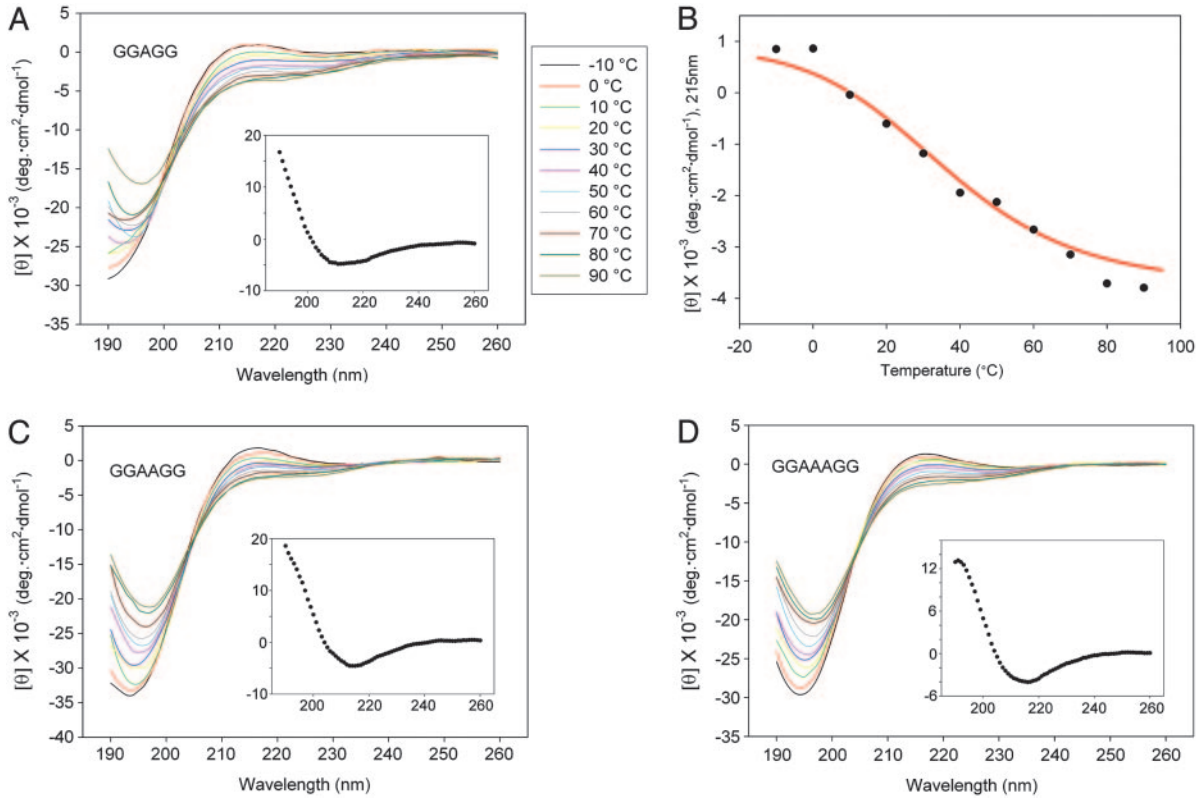

Fig. 1. CD spectroscopy of the peptides of this study. (*A*) Far-UV CD spectra of GGAGG. (*B*) The transition curve of GGAGG from CD 215 nm absorbance. The fit curve is shown in red. (*C*) Far-UV CD spectra of GGAAGG. (*D*) Far-UV CD spectra of GGAAAGG. The *Insets* in *A*, *C*, and *D* show the difference spectra between −10°C and 90°C.

possible to read coupling constants directly from the splitting of the amide proton to a precision of ±0.03 Hz on average.

2D NOESY (34) experiments were carried out on samples of 2-mM unlabeled GGAGG in the same buffer as the 1D NMR and CD measurements. The pulse sequence is the standard NOESYGPPH19 in the Bruker sequence library, with the modification of adding a homospoil Z-gradient pulse during the recycle delay. The mixing time was optimized as 100 ms to minimize spin diffusion effects and COSY artifacts. Spectral widths were 6,000 Hz in both dimensions. A set of 4,096 complex data points was collected in the t2 domain, and 256 t1 time increments were acquired in States-time-proportional phase incrementation (TPPI) mode (35). The assignments were carried out by the analysis of 2D total correlation spectroscopy (TOCSY) (36) and NOESY spectra. Chemical shifts were calibrated with 2,2-dimethylsilapentane-5-sulfonic acid (DSS). All four temperature (−10°C, 0°C, 20°C, and 40°C) NOESY data sets were processed by the same NMRPIPE (37) 2D process script, and nuclear Overhauser effect (NOE) cross-peaks were integrated by using SPARKY (T. D. Goddard and D. G. Kneller, University of California, San Francisco). A 30% integration error in NOE peak volumes will propagate to an error of ±0.4 in the NOE ratio.

NOE Simulations. Atomic coordinates of GGAGG were built with the Biopolymer module in INSIGHTII (Accelrys, San Diego). A Fortran code was written to rotate the Ψ angle of the Ala-3 CA-CO bond in 5° increments from −175° to 175° whereas the Φ angle is held at −70°, −75°, and −80°, respectively. The methyl group is represented by a pseudoatom located at the geometric center of three methyl protons. The distances were recorded for every rotation. NOE intensities were calculated from the inverse sixth power relationship to distance based on the assumption of a uniform relaxation rate for each proton. In calculating NOE distances, the 2.96-Å distance between Hβ of N-terminal acetyl group and HN Gly-1 was used as a fixed reference.

Results

Secondary Structure Observed from CD Spectroscopy. Far-UV CD spectroscopy shows that PII structure dominates in all GG(A)nGG peptides at low temperatures (Fig. 1 *A*, *C*, and *D*), based on the strong negative band at 195 nm and weak positive band at 215 nm (38). The high temperature *U* state differs from *P* in that the intensity of the 195-nm negative band increases and that of the 215-nm positive band decreases. The difference spectra between high and low temperatures shown as inserts in Fig. 1 *A*, *C*, and *D* are consistent with a β-like CD curve, sharing a common negative band at 210–220 nm but differing in the relative intensity of the positive band at 195 nm (39). Thus, the major change in conformation at high temperature seems to be an increase in β-like structure. We argue below that this structure probably differs from canonical β. The appearance of clearly defined isodichroic points at 203 nm in the spectra of GGAAGG (Fig. 1*C*) and GGAAAGG (Fig. 1*D*) peptide is consistent with two-state overall transition behavior: i.e., a given alanine is either *P* or *U* (see below). The isodichroic point in GGAGG is less well defined (Fig. 1*A*), but only the 90°C data deviate. Because the CD data for GGAGG level off at low and high temperatures (Fig. 1*B*), we assume that the low and high temperature $^3J_{\alpha N}$ values from NMR data span a reasonable fraction of the *P*–*U* transition in each peptide.

Thermodynamic Results from NMR $^3J_{\alpha N}$ Measurement of GGA*GG. A transition curve is shown in Fig. 2*A* for $^3J_{\alpha N}$ of GGA*GG (the

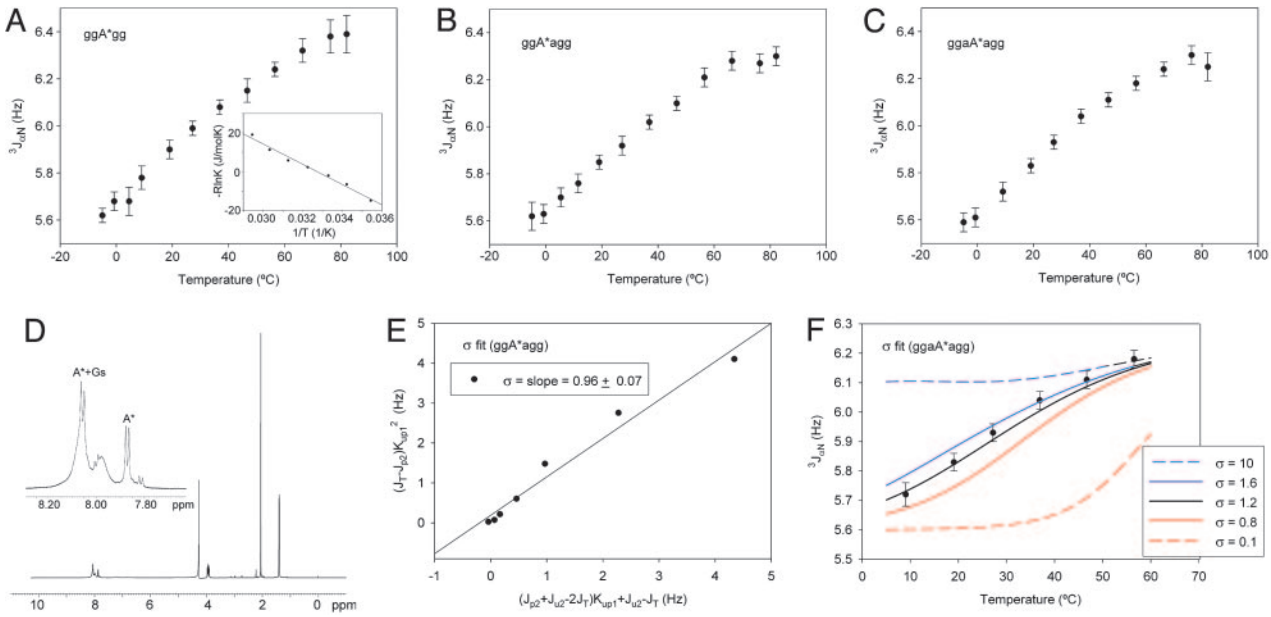

Fig. 2. NMR spectroscopy results and related data analysis of peptides of this study. (*A–C*) Transition curves observed by $^{3}J_{\alpha N}$ measurement. (*A*) GGA*GG (the asterisk representing ^{15}N labeling). (*Inset*) A thermodynamic plot (Eq. **7**). (*B*) GGA*AGG. (*C*) GGAA*AGG. (*D*) 1D high-resolution proton NMR spectrum of GGA*GG at 80°C. (*Inset*) The enlarged amide region. (*E*) A linear regression fit plot of Eq. **9** using data in *B*. (*F*) The σ fitting plots of Eq. **11** using data in *C*.

asterisk represents ^{15}N labeling) from 0°C to 80°C. Estimating *Jp* and *Ju* to be 5.68 and 6.39 Hz, respectively, K_{up1} can be evaluated at each temperature from Eqs. **1** and **2**. ΔH_{up1} is then obtained from the slope of a linear regression plot (Eq. **3**, Fig. 2*A Inset*) as -52.3 kJ·mol^{-1}. Finally a ΔS_{up1} value of -171 J·mol^{-1}·K^{-1} is estimated from the intercept of the *y* axis in the same regression line as $1/T$ approaches zero. So, for GGAGG

$$-RT\ln K_{up1} = -5.23 \times 10^4 - T(-171). \qquad [7]$$

We believe this high enthalpy value is unreliable. R. W. Woody (personal communication) has previously pointed out that the apparent heat of 52.3 kJ·mol^{-1} drops to ≈13 kJ·mol^{-1} if 10%–15% of the high-temperature *U* state is present at 0°C, which seems realistic (25). The fact that H-bonded water structure may be significantly disrupted at high temperature contributes to the enthalpy change in addition to peptide hydration. Baldwin (40) recently predicted the electrostatic solvation free energy for a PII alanine residue to be -9.1 kcal·mol^{-1} referenced to a fully buried residue (40) and -0.8 kcal·mol^{-1} referenced to a canonical β structure (41). Finally, we have ignored any ΔC_p effects in fitting the enthalpy.

Thermodynamics from CD Spectroscopy. We carried out a parallel analysis of the CD data for GGAGG, using values at 215 nm (Fig. 1*B*). The resulting enthalpy change $\Delta H_{up1} = -42.3$ kJ·mol^{-1} and entropy change $\Delta S_{up1} = -137$ J·mol^{-1}·K^{-1} agree roughly with the values derived from NMR (<20% differences in parameters are reasonable in van't Hoff analysis). Whereas the CD spectra are remarkably sensitive to subtle changes in backbone geometry, they cannot report on individual residues in the conformational ensemble. Thermodynamic analysis of the CD spectral data for the longer peptides also requires knowledge of the dependence of the CD signal on chain length. On the other hand, the NMR coupling constants are localized to individual residues. For this reason, we have pursued analysis of cooperativity by using the NMR data only.

Cooperativity Calculated from Coupling Constants of GGA*AGG and GGAA*AGG. The transition curve of the Ala-3 residue in GGA*AGG (Fig. 2*B*) allows assessment of the cooperativity relative to the isolated alanine residue in GGAGG. *Jp2* and *Ju2* are taken as 5.63 and 6.28 Hz, respectively. The theoretical expression for $J_{(T)}$ of residue Ala-3 in GGA*AGG is (see Table 1):

$$J_{(T)} = J_{p2} \times \frac{\sigma s + \sigma s^2}{1 + 2\sigma s + \sigma s^2} + J_{u2} \times \frac{1 + \sigma s}{1 + 2\sigma s + \sigma s^2}. \qquad [8]$$

Replacing $K_{up1} = \sigma s$ from Eq. **5** and rearranging Eq. **8** above, we get

$$(J_{(T)} - J_{p2})K_{up1}{}^2 = \sigma[(J_{p2} + J_{u2} - 2J_{(T)})K_{up1} + J_{u2} - J_{(T)}]. \qquad [9]$$

By calculating $K_{up1}(T)$ from Eq. **7** at each temperature, the value of σ is obtained by linear regression of both sides of the equation above, which gives a σ of 0.96 ± 0.07 (Fig. 2*E*).

Analysis of the transition curve for the Ala-4 residue in GGAA*AGG (Fig. 2*C*) gives comparable values. *Jp3* and *Ju3* values are set at 5.60 and 6.26 Hz, respectively, according to the curve. The theoretical expression for $J_{(T)}$ of residue Ala-4 in GGAA*AGG is (see Table 1):

$$J_{(T)} = J_{p3} \times \frac{\sigma s + \sigma s^3 + 2\sigma s^2}{1 + 3\sigma s + 2\sigma s^2 + \sigma^2 s^2 + \sigma s^3} + J_{u3} \times \frac{1 + \sigma^2 s^2 + 2\sigma s}{1 + 3\sigma s + 2\sigma s^2 + \sigma^2 s^2 + \sigma s^3}. \qquad [10]$$

After substituting $K_{up1} = \sigma s$, we have

$$J_{(T)} = \frac{(K_{up1}\sigma^2 + 2K_{up1}^2\sigma + K_{up1}^3) \times J_{p3} + [(K_{up1} + 1)^2\sigma^2] \times J_{u3}}{(K_{up1}^2 + 3K_{up1} + 1)\sigma^2 + 2K_{up1}^2\sigma + K_{up1}^3}. \qquad [11]$$

Table 1. Statistical weights of conformational states in GG(A)nGG peptides

Peptide	PII residues	Statistic weight
$(A)_1$		
U	0	1
P	1	σs
$(A)_2$		
UU	0	1
UP	1	σs
PU	1	σs
PP	2	σs^2
$(A)_3$		
UUU	0	1
UUP	1	σs
UPU	1	σs
PUU	1	σs
UPP	2	σs^2
PPU	2	σs^2
PUP	2	$\sigma^2 s^2$
PPP	3	σs^3

By calculating $K_{up1}(T)$ from Eq. **7** and varying σ from 0.8 to 1.6, the best fit of σ to experimental data is found to be 1.2 (Fig. 2*F*).

Time-Averaged Conformation of GGAGG During *P–U* Transition. During the *P–U* transition, the averaged Φ angle of alanine in GGAGG, calculated from a Karplus relation (42, 43), lies between $-70°$ and $-80°$ ($^3J_{\alpha N} \approx 5$–6 Hz) (see Fig. 4*A*). To define Ψ, we apply a ratio method using NOE data (10, 25). Briefly, the ratio of NOE intensities between the protons of Hβ Ala-3 and their own HN to that between Hβ Ala-3 and the succeeding Gly-4 HN is sensitive to each Φ/Ψ point on the Ramachandran plot. The NOE ratio corresponding to PII is 4.1; the NOE ratios for β structure range from 1 to 8. The observed ratio drops from 7.2 to 1.7 as temperature increases from 0°C to 40°C (Fig. 3, Table 2). Simulation of the NOE ratios (Fig. 4*B*) indicates that the average Ψ angle increases from $+120°$ to $+170°$ within the estimated Φ angle range from $-70°$ to $-80°$. At 40°C, the averaged alanine conformation ($\Phi = -80°$, $\Psi = +170°$) clearly deviates from canonical PII structure on the Ramachandran plot.

An alternative explanation for an NOE ratio of 7.2 corresponds to Ψ angles close to 0° (Fig. 4*B*), which is not in a normally allowed region of the Ramachandran plot (44, 45). An NOE ratio of 1.7 corresponds to α-helix, inconsistent with the increase in $^3J_{\alpha N}$ and lack of observable $d_{NN(i,i+1)}$ NOEs under all conditions.

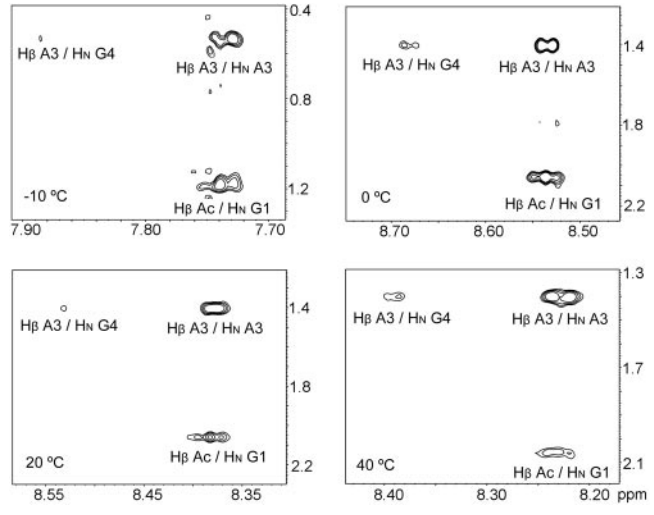

Fig. 3. Selected areas of 2D NOESY spectra of GGAGG recorded at the indicated four different temperatures.

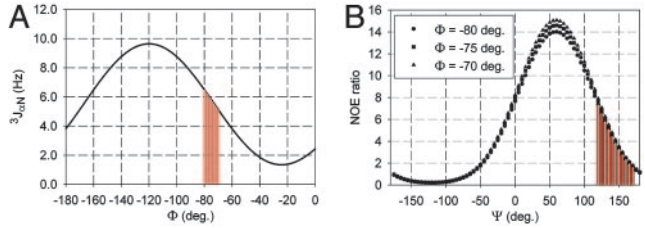

Fig. 4. Conformational analysis of GGAGG by NMR. (*A*) A plot of $^3J_{\alpha N}$ vs. Φ using Bax's parameters. (*B*) The simulated NOE ratios. The red bar area corresponds to the averaged conformations of GGAGG defined by NMR measurements from 0°C to 40°C.

Discussion

Absence of Cooperativity in PII Structure Formation. The main conclusion from this analysis is that the PII structure in the shortest oligomers of alanine is noncooperative, within our experimental determination of $\sigma = 1 \pm 0.2$. Pappu and Rose (23) and Pappu *et al*. (27) predicted this result based on the fact that Flory's (45) isolated pair model holds for the PII region. This result has several additional implications. Any water interactions with the peptide backbone as modeled by the alanine side chain are local, and, whereas extended bridges of the kind seen in collagen peptide structures may exist, they do not contribute energetically. Garcia (9) predicted the existence of a hydration groove in chains of 5–6 consecutive PII alanine residues that might enhance cooperativity because of direct water peptide H-bonding. This result is similar to the minor groove hydration of B-DNA, which can be demonstrated directly by NMR analysis of NOE/rotating-frame Overhauser effect (ROE) ratios (46) and magnetic relaxation dispersion (MRD) (47). Hydration experiments on our PII peptides using NOE/ROE ratio analysis reveal no significant difference from the cyclic oxytocin case (48), giving no indication for a stable hydration groove. The signs of NOEs in a solvent-solute cross-relaxation study on a collagen-like peptide also suggest a kinetically labile hydration shell (49). We infer from the present study and these preliminary hydration data that PII hydration is not as extended or as stable as that in DNA duplexes where longer range electrostatic interactions occur along the backbone. Longer PII peptides could be studied by MRD to try to detect Garcia's hydration groove.

If the lack of cooperativity for PII in Ala sequences holds generally, the analysis of *U* states in proteins is greatly simplified. Consider the helix–"coil" transition in poly(Ala). According to Zimm and Bragg (28), the statistical weight of coil is set to unity, as a reference. If we equate the fully unfolded state with *U*, and weigh this as unity, the lack of cooperativity in *U* allows us to reinterpret the constant *s* for adding a helical residue to the end

Table 2. Experimental NOE ratios and NOE distances in GGAGG at four temperatures

		NOE distance, Å	
Temperature, °C	NOE ratio	Ala3Hβ-Ala3HN	Ala3Hβ-Gly4HN
−10	6.5 ± 0.4	3.12	4.26
0	7.2 ± 0.4	2.74	3.81
20	4.7 ± 0.4	3.02	3.91
40	1.7 ± 0.4	2.84	3.10

of a nucleated helix as $s' = s(1 + K_{up})$, where s is the original ZB propagation constant and K_{up} is the equilibrium constant for the transition from U to P. This adjustment means that a simple rescaling of the ZB s value suffices to describe the α–P–U transition in poly(Ala). It is, of course, crucial to know whether all side chains behave like Ala.

Finally, flanking glycines do not perturb either the steric or solvent interactions of the alanines in these models (50). One reservation that has been expressed concerning the presence of glycine in model peptides is that its extended conformational range might serve to perturb the conformations of vicinal side chains. That is, glycines in certain regions of their enlarged Φ and Ψ space might exclude some of the phase space of flanking side chains. This issue seems not to be a factor in the case of alanine, although there may indeed be such effects in longer side chains. One possible explanation for the lack of such an effect in alanine is that, whereas the conformational space accessible to glycine is indeed extensive relative to any other side chains, steric clashes resulting from its presence in normally excluded domains of phase space are "soft" because glycine has no strong preference for any particular values.

The High-Temperature State in GG(A)nGG Peptides. The fact that the CD spectra and NMR $^3J_{\alpha N}$ coupling constants are temperature-sensitive has been interpreted to indicate that alanine in either GGAGG or $X_2A_7O_2$ shifts from a predominantly PII to a more β-like conformation as temperature increases (10, 25). The same results are obtained now for our model GG(A)nGG peptides (Figs. 1 and 2). The U state is distinct from canonical PII structure as seen by disappearance of the 215-nm positive band in the CD spectra (Fig. 1), accompanied by significant NOE ratio changes (Fig. 3, Table 2). The CD difference spectra are qualitatively consistent with acquisition of β-like structure. Garcia's (9) high-temperature 10-ns molecular dynamics simulation of an Ala-21 peptide predicts that disordered structures favored at high temperature consist of a blend of PII, β, and α (9). We detect little α structure in CD or NOESY spectra. In their pioneering analysis of this problem, Tiffany and Krimm (19) supposed that, at a high enough temperature, a statistical random coil-like conformation can be attained. None of these models satisfactorily explains the temperature-dependent CD curves and plateau signal in the coupling constants at temperatures around 80°C. Any fraction of α-helix present at low temperature would be expected to diminish at high temperature (51). We believe the high-temperature state (here labeled as U) corresponds to an extended β-like conformation. At 40°C, the averaged conformation ($\Phi = -80°$, $\Psi = +170°$) of GGAGG corresponds to an equilibrium between canonical PII and a structure having dihedral angles within the extended β area. The barrier between P and U is presumably due to differential hydration effects and/or hyperconjugation, as suggested by Hinderaker and Raines (52). It seems reasonable to suppose that thermodynamic differences among states within the U or extended β ensemble are small enough to justify grouping them collectively as a "state" (53). We use U rather than β to emphasize that U need not correspond in detail to canonical β structure.

We thank Buzz Baldwin, Clay Bracken, Zhengshuang Shi, and Alex Vologodskii for helpful discussions. This work was supported by the Office of Naval Research.

1. Dunker, A. K., Brown, C. J. & Obradovic, Z. (2002) *Adv. Protein Chem.* **62,** 25–49.
2. Baldwin, R. L. (2002) *Adv. Protein Chem.* **62,** 361–367.
3. Tanford, C. (1968) *Adv. Protein Chem.* **23,** 121–282.
4. Shi, Z., Woody, R. W. & Kallenbach, N. R. (2002) *Adv. Protein Chem.* **62,** 163–240.
5. Eker, F., Cao, X., Nafie, L., Huang, Q. & Schweitzer-Stenner, R. (2003) *J. Phys. Chem. B.* **107,** 358–365.
6. McColl, I. H., Blanch, E. W., Hecht, L., Kallenbach, N. R. & Barron, L. D. (2004) *J. Am. Chem. Soc.* **126,** 5076–5077.
7. Schweitzer-Stenner, R., Eker, F., Griebenow, K., Cao, X. & Nafie, L. A. (2004) *J. Am. Chem. Soc.* **126,** 2768–2776.
8. Gnanakaran, S. & Garcia, A. E. (2003) *J. Phys. Chem. B* **107,** 12555–12557.
9. Garcia, A. E. (2004) *Polymer* **45,** 669–676.
10. Ding, L., Chen, K., Santini, P. A., Shi, Z. & Kallenbach, N. R. (2003) *J. Am. Chem. Soc.* **125,** 8092–8093.
11. Wüthrich, K. (1986) *NMR of Proteins and Nucleic Acids* (Wiley, New York), pp. 14–19.
12. Plaxco, K. W., Morton, C. J., Grimshaw, S. B., Jones, J. A., Pitkeathly, M., Campbell, I. D. & Dobson, C. M. (1997) *J. Biomol. NMR* **10,** 221–230.
13. van der Spoel, D. (1998) *Biochem. Cell Biol.* **76,** 164–170.
14. Nelson, J. W. & Kallenbach, N. R. (1986) *Proteins* **1,** 211–217.
15. Luo, P. & Baldwin, R. L. (1997) *Biochemistry* **36,** 8413–8421.
16. Liu, Z., Chen, K., Ng, A., Shi, Z., Woody, R. W. & Kallenbach, N. R. (2004) *J. Am. Chem. Soc.*, in press.
17. Tobias, D. J. & Brooks, C. L. I. (1992) *J. Phys. Chem.* **96,** 3864–3870.
18. Bolhuis, P. G., Dellago, C. & Chandler, D. (2000) *Proc. Natl. Acad. Sci. USA* **97,** 5877–5882.
19. Tiffany, M. L. & Krimm, S. (1968) *Biopolymers* **6,** 1379–1382.
20. Adzhubei, A. A. & Sternberg, M. J. (1993) *J. Mol. Biol.* **229,** 472–493.
21. Kramer, R. Z., Vitagliano, L., Bella, J., Berisio, R., Mazzarella, L., Brodsky, B., Zagari, A. & Berman, H. M. (1998) *J. Mol. Biol.* **280,** 623–638.
22. Han, W. G., Jalkanen, K. J., Elstner, M. & Suhai, S. (1998) *J. Phys. Chem. B.* **102,** 2587–2602.
23. Pappu, R. V. & Rose, G. D. (2002) *Protein Sci.* **11,** 2437–2455.
24. Drozdov, A. N., Grossfield, A. & Pappu, R. V. (2004) *J. Am. Chem. Soc.* **126,** 2574–2581.
25. Shi, Z., Olson, C. A., Rose, G. D., Baldwin, R. L. & Kallenbach, N. R. (2002) *Proc. Natl. Acad. Sci. USA* **99,** 9190–9195.
26. Stapley, B. J. & Creamer, T. P. (1999) *Protein Sci.* **8,** 587–595.
27. Pappu, R. V., Srinivasan, R. & Rose, G. D. (2000) *Proc. Natl. Acad. Sci. USA* **97,** 12565–12570.
28. Zimm, B. H. & Bragg, J. K. (1959) *J. Chem. Phys.* **31,** 526–535.
29. Scholtz, J. M., Qian, H., York, E. J., Stewart, J. M. & Baldwin, R. L. (1991) *Biopolymers* **31,** 1463–1470.
30. Piotto, M., Saudek, V. & Sklenar, V. (1992) *J. Biomol. NMR* **2,** 661–665.
31. Troganis, A. N., Tsanaktsidis, C. & Gerothanassis, I. P. (2003) *J. Magn. Reson.* **164,** 294–303.
32. Pople, J. A. (1958) *Mol. Phys.* **1,** 168–174.
33. McConnell, J. (1987) *The Theory of Nuclear Magnetic Relaxation in Liquids* (Univ. of Cambridge Press, Cambridge, U.K.), pp. 113–126.
34. Kumar, A., Ernst, R. R. & Wüthrich, K. (1980) *Biochem. Biophys. Res. Commun.* **95,** 1–6.
35. Keeler, J. & Neuhaus, D. (1985) *J. Magn. Reson.* **63,** 453–472.
36. Bax, A. & Davis, D. G. (1985) *J. Magn. Reson.* **65,** 355–360.
37. Delaglio, F., Grzesiek, S., Vuister, G. W., Zhu, G., Pfeifer, J. & Bax, A. (1995) *J. Biomol. NMR* **6,** 277–293.
38. Sreerama, N. & Woody, R. W. (1994) *Biochemistry* **33,** 10022–10025.
39. Tilstra, L. & Mattice, W. L. (1996) in *Circular Dichroism and the Conformational Analysis of Biomolecules*, ed. Fasman, G. D. (Plenum, New York), pp. 261–284.
40. Baldwin, R. L. (2003) *J. Biol. Chem.* **278,** 17581–17588.
41. Avbelj, F. & Baldwin, R. L. (2004) *Proc. Natl. Acad. Sci. USA* **101,** 10967–10972.
42. Karplus, M. (1959) *J. Chem. Phys.* **30,** 11–15.
43. Vuister, G. W. & Bax, A. (1993) *J. Am. Chem. Soc.* **115,** 7772–7777.
44. Ramachandran, G. N., Ramakrishnan, C. & Sasisekharan, V. (1963) *J. Mol. Biol.* **7,** 95–99.
45. Flory, P. J. (1969) *Statistical Mechanics of Chain Molecules* (Interscience, New York).
46. Jacobson, A., Leupin, W., Liepinsh, E. & Otting, G. (1996) *Nucleic Acids Res.* **24,** 2911–2918.
47. Denisov, V., Carlstrom, G., Venu, K. & Halle, B. (1997) *J. Mol. Biol.* **268,** 118–136.
48. Modig, K., Liepinsh, E., Otting, G. & Halle, B. (2004) *J. Am. Chem. Soc.* **126,** 102–114.
49. Melacini, G., Bonvin, A. M. J. J., Goodman, M., Boelens, R. & Kaptein, R. (2000) *J. Mol. Biol.* **300,** 1041–1048.
50. O'Connell, T. M., Wang, L., Tropsha, A. & Hermans, J. (1999) *Proteins* **36,** 407–418.
51. Lopez, M. M., Chin, D.-H., Baldwin, R. L. & Makhatadze, G. I. (2002) *Proc. Natl. Acad. Sci. USA* **99,** 1298–1302.
52. Hinderaker, M. P. & Raines, R. T. (2003) *Protein Sci.* **12,** 1188–1194.
53. Shortle, D. (2003) *Protein Sci.* **12,** 1298–1302.